The Influence of Segregation of Mn on the Recrystallization Behavior of C-Mn Steels

C. SLATER, A. MANDAL, and C. DAVIS

The influence of Mn segregation that occurs during casting on recrystallization kinetics has been explored for a C-Mn automotive steel. A homogenization heat treatment was used to remove Mn segregation, while maintaining a similar initial austenite grain size to the segregated condition, to provide base-line comparison data. Deformation trials were carried out in a Gleeble thermomechanical simulator to 0.3 strains at 900 °C, and significant differences in both recrystallization times and final grain sizes were seen between the two conditions. The segregated sample incurred a longer recrystallization time and a wider recrystallized grain size distribution than the homogenized sample. A finite element model was used to predict the local deformation strains based on variations in material properties caused by segregation; the model used data from XRF elemental mapping of Mn to define the local mechanical properties based on differences in solid solution strengthening. Local strain variations ranging from 0.19 to 0.49 were predicted in the segregated sample for an overall applied 0.3 strain (compared to 0.26 to 0.35 in the homogenized sample); using these strains to predict the recrystallized grain sizes gave a much better prediction for the grain size distribution.

https://doi.org/10.1007/s11663-019-01603-2

I. INTRODUCTION

RECRYSTALLIZATION in steel still remains one of the key approaches to refining grain structure during steel production and has been studied for many decades.[1–3] Empirical equations, such as the Dutta–Sellars model,[4,5] developed to predict recrystallization behavior, are widely used and provide an understanding of the governing mechanisms and sensitivities that define the recrystallization rate and final recrystallized grain size. The demand for improving properties of materials continues and, thus, there is a need to increase the accuracy in prediction of the full grain structure as this affects strength and toughness. Recently, full grain size distributions, rather than mode size,[6] have been used in recrystallization modeling, and it is known that the fine grains recrystallize first followed by the larger grains in the distribution, with the largest grains in the distribution having the biggest influence on toughness. Ensuring that the extremes of the grain size distribution are correctly represented in terms of recrystallization will help process optimization and product development. An aspect that has not yet been considered is the effect that segregation during casting might have on the recrystallization kinetics and grain size during hot deformation.

Many steels display the effects of casting in the form of segregation, for example, in microstructural banding of the ferrite and martensite in dual-phase steels[7] and in inhomogeneous Nb precipitation in HSLA steel,[8] to name just two. In common, C-Mn automotive forging grades segregation can be seen by local variations in Mn and Cr levels, and a banded ferrite + pearlite structure in the soft condition.[9] Mn is known to have in impact on solid solution strengthening with the empirical equations for strengthening indicating a typical increase in yield strength of 32 to 43 MPa/wt pct Mn in ferrite.[10] Cr, on the other hand, has little to no impact on the solution strengthening of steel.[11] Differences in local strength levels will have an effect during deformation, for example, *via* strain inhomogeneity during hot rolling or forging. This in turn may have a significant impact on recrystallization behavior due to the strong sensitivity of recrystallization time (ε^4) and recrystallized grain size (ε^{-1}) to strain,[3] and is the subject of this paper.

C. SLATER, A. MANDAL, and C. DAVIS are with the University of Warwick, Coventry, CV4 7AL, U.K. Contact e-mail: c.d.slater@warwick.ac.uk

Manuscript submitted November 20, 2019.
Article published online May 15, 2019.

II. METHODOLOGY

For this study, a 20MnCr5-type steel, supplied by Liberty Speciality Steel, used in the automotive industry for forged components was used (composition in Table I). The as-received material was commercially air-melted ingot, reheated, and rolled and forged to 90-mm bar stock representative of automotive feedstock. This bar was sectioned to two 5 cm cubes from the ½ radius; an as-received condition (referred to as the "segregated sample" henceforth) and one section which was heat treated for homogenization. The homogenization heat treatment consisted of three thermal cycles involving heating to 900 °C initially, then cycling between 900 °C and 400 °C at 2 °C/s before cooling to room temperature (a schematic of this can be seen in Figure 1, after which the sample was air cooled to room temperature). The objective of the heat treatment was to use the phase transformation between austenite and ferrite + pearlite to redistribute the Mn (and Cr) from the initial segregation distribution as it is known that Mn is swept along with the transformation front.[12] The low (900 °C) austenitization temperature was selected to minimize grain growth so that a grain size similar to that of the as-received sample could be obtained.

A Bruker M4 Tornado micro XRF was used to composition map the cross sections of both the as-received and homogenized samples using a spot size of 20 μm and a spacing of 15 μm.

A Gleeble HDS-V40 thermomechanical simulator was used for recrystallization trials. All tests were carried out in a vacuum of 5×10^{-3} mbar. Rods of 10 mm in diameter by 15 mm in length, machined from the segregated and homogenized samples, were heated to 1100 °C at the rate of 20 °C/s and held for 5 minutes. The sample was then cooled to 900 °C at the rate of 10 °C/s, held for 30 seconds before being subjected to a compressive strain of 0.3 at a strain rate of 1 s^{-1}; tests with varying post deformation holding times ranging from 30 to 300 seconds were carried out prior to an air quenching at the rate of approximately 70 °C/s to room temperature. A schematic of the three different Gleeble profiles used is shown in Figure 2.

An additional sample of both the segregated and homogenized samples were also heated to 1100 °C and held for 5 minutes before quenching in order to measure the prior austenite grain size just prior to deformation for both conditions.

Another set of experiments was performed in order to determine that no significant grain growth occurred after recrystallization. Samples were taken directly after the homogenization stage of the Gleeble heat treatment (Figure 1), which had a mode size of prior austenite grain size of 20 μm, and were heat treated in a Carbolite RHF 15/8 chamber furnace at 900 °C in air for 30, 60, 90, and 120 minutes before quenching in a water bath.

All samples were sectioned along the longitudinal axis and polished to a 0.5 μm finish. The samples were then etched in Picric solution (2g Picric Acid, 100ml Ethanol, and 2 drops of HCl) for 5 minutes at room temperature. Prior austenite grain sizes were measured in all samples as an equivalent circle diameter, where a minimum of 300 grains were measured for each condition.

Table I. Composition of the Steel Used in This Study (All Wt Pct)

Fe	C	Si	Mn	Cr	P	S
Bal.	0.176	0.285	1.2	1.25	0.003	0.006

III. RESULTS AND DISCUSSION

Figure 3 shows the Mn Micro XRF traces for the segregated and homogenized samples. The segregated sample, Figure 1(a), shows a characteristic banding distribution in the rolling direction, which is related to the initial interdendritic segregation from casting and rolling reduction. The banding spacing is approximately 200-250 μm, which arises from segregation in the initial

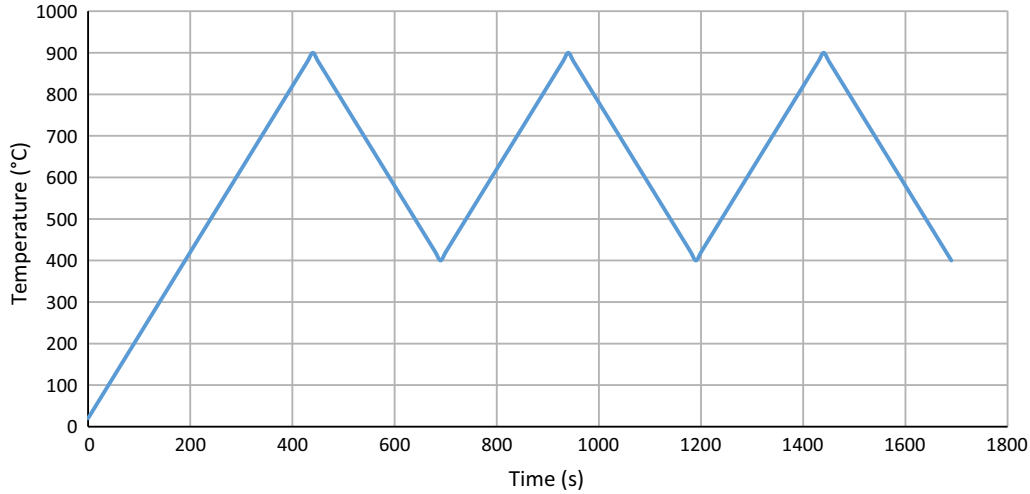

Fig. 1—Schematic diagram showing the thermal profile used to homogenize the segregated sample.

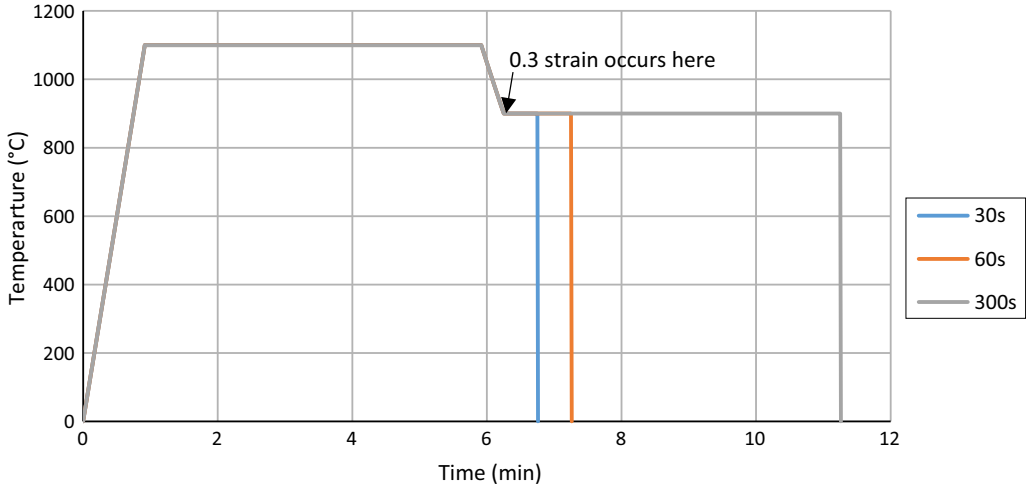

Fig. 2—Schematic diagram showing the three different thermal profiles used in Gleeble.

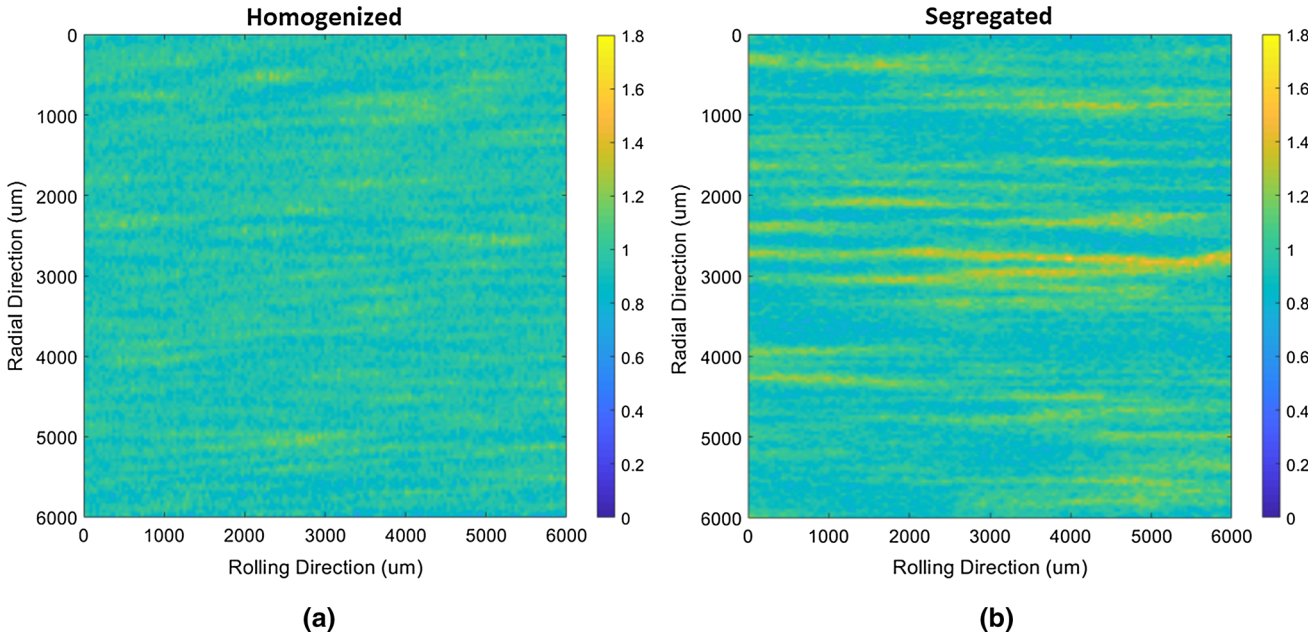

Fig. 3—Micro XRF traces for Mn content (color scale in wt pct) in (*a*) the homogenized sample and (*b*) the segregated sample. An error of around 0.1 wt pct Mn should be taken into consideration with this method.

210-mm-thick cast ingot with rolling/forging to the 90 mm bar. The segregation level can be seen to reach 1.8 wt pct Mn in the interdendritic regions to 0.6 wt pct Mn in the dendritic regions. This agrees well with the levels reported in the literature[12–14] where Mn variations of between 2 and 4 times between interdendritic and dendritic regions have been reported in the as-cast/semifinished states. It can clearly be seen that the segregation profile in the homogenized sample is reduced, Figure 3(b), with peak values decreasing to around 1.28 wt pct Mn and the minimum values being around 0.9 wt pct Mn. This gives a significantly reduced range of 0.38 wt pct Mn compared to 1.2 wt pct Mn in the segregated sample. The banded structure has been significantly reduced in the homogenized sample. It should also be noted that Cr also segregated to a similar level in these steels (0.8 to 1.9 in the segregated sample and 1 to 1.35 in the homogenized); however, due to the limited impact that Cr has on solid solution strengthening, the remainder of the paper focuses on solely Mn distribution.

Analysis of samples heat treated at 900 °C for 30, 60, 90, and 120 minutes revealed that the mode grain size grew to 20, 20, 22, and 24 μm, respectively (from the initial 20 μm mode grain size). This shows that, for grains as small as 20 μm at the deformation temperatures tested here, no significant grain growth is expected, and the measured grain size is in the as-recrystallized state.

Prior to deformation testing, segregated and homogenized samples were heated to 1100 °C for 5 minutes and quenched to martensite in order to observe the prior austenite grain structure. This was done to ensure that the grain size distributions are as similar as possible such that any differences during recrystallization could be ascribed to the segregation levels. The prior austenite grain size distributions can be seen in Figure 4. Both the samples show a mode grain size in the range of 170 to 190 μm. The homogenized sample shows a slightly coarser grain size distribution (by about 20 μm). Due to the nature of the homogenization process, the cyclic heating acts to normalize and refine the microstructure. However, the reduced segregation can also lead to a reduced level of solute drag on the boundaries. Therefore, the times and temperatures seen in Figure 1 are optimized to obtain the minimal discrepancy as shown in Figure 4.

To determine if Mn segregation affects the recrystallization behavior in these steels (due to local variations in strength level causing strain inhomogeneity during deformation and its consequent effect on recrystallization kinetics and grain size development) hot deformation tests with varying hold times after deformation were carried out. A strain of 0.3 was selected because: this is below the level expected to cause dynamic recrystallization in C-Mn steels (reported to be around a strain of 0.45[3]) even if local strain variation occurs; 0.3 strain results in a significant amount of grain refinement (as seen from Eq. [1]); and 0.3 strain is widely experienced during industrial processing of C-Mn steels, particularly during hot rolling.

Figure 5 shows the austenite grain size distribution for both the segregated and homogenized samples after deformation to a strain of 0.3 at 900 °C, and held there for 30 seconds before quenching. The final recrystallized grain size can be predicted by the following equation for C-Mn steels[3]:

$$D_{\mathrm{SRX}} = D' D_0^{0.674} \varepsilon^{-1}, \qquad [1]$$

where D_{SRX} the grain size after static recrystallization and D' a material constant (with fitted values between 0.35 and 0.74[3,15–18] have been reported; here, a value of 0.57 to fit to the mode grain size for the homogenized sample was found to be appropriate.).

For C-Mn steels, the recrystallization kinetics can be described by the following equations[3]:

$$\mathrm{Rs} = 6.75 \times 10^{-20} \varepsilon^{-4} D_0^2 \exp\left(\frac{Q}{RT}\right). \qquad [2]$$

$$0.85 = 1 - \exp\left(\ln(0.95)\left(\frac{\mathrm{Rf}}{\mathrm{Rs}}\right)\right)^2, \qquad [3]$$

where Rs and Rf are the times for 5 and 85 pct static recrystallizations, respectively, ε is the strain, D_0 is the original grain size, and Q is the activation energy of recrystallization (reported to vary between 100 and 285 kJ mol^{-1} for C-Mn steel,[19] and 276 kJ mol^{-1} was used in this study based on a similar steel composition and initial grain size used in.[19] Using Eqs. [2] and [3], a time for 85 pct recrystallization between 8 and 11 seconds is predicted for this steel, assuming uniform Mn levels, *i.e.*, no segregation (based on using a mode grain size of 170 or 190 μm).

A noticeable difference in the two grain size distributions after holding for 30 seconds following 0.3 strain is readily seen in Figure 5 (typical micrographs of the prior austenite grain boundaries etched in the martensite are given in Figure 6). The homogenized sample has fully recrystallized and produced a mode grain size of 62 μm with a tight distribution (range 20 to 140 μm). These results agree well with the predictions for 85 pct recrystallization to occur within 11 seconds. The

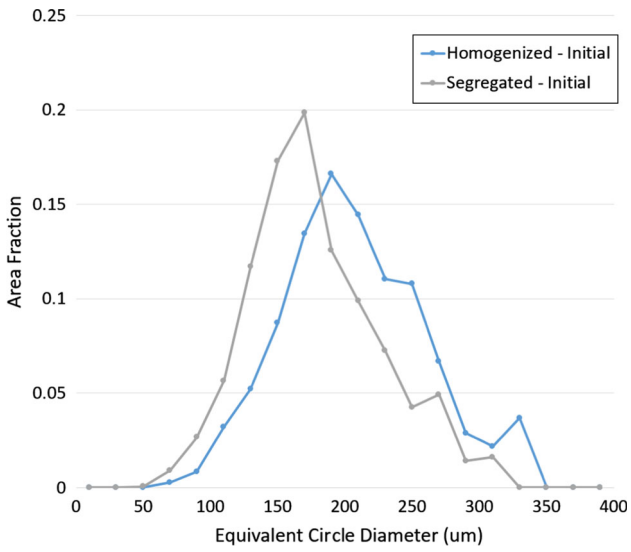

Fig. 4—Initial austenite grain distribution for the segregated sample and homogenized sample after 5 min at 1100 °C followed by quenching.

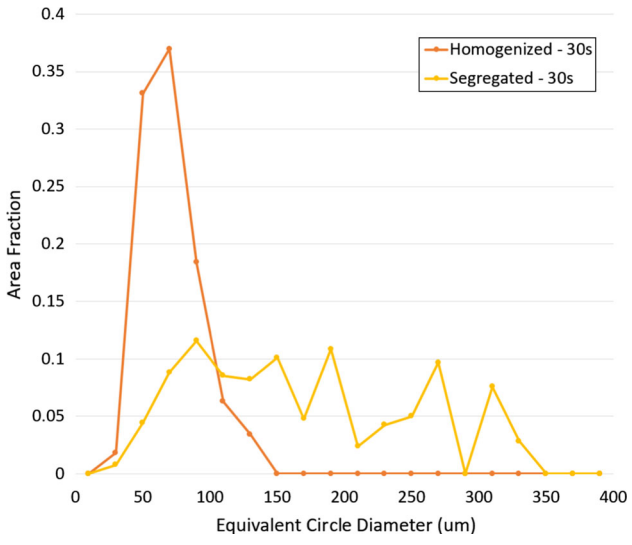

Fig. 5—Austenite grain size distribution for both the homogenized and segregated samples after being deformed to 0.3 strain at 900 °C and held for 30 s before air quenching.

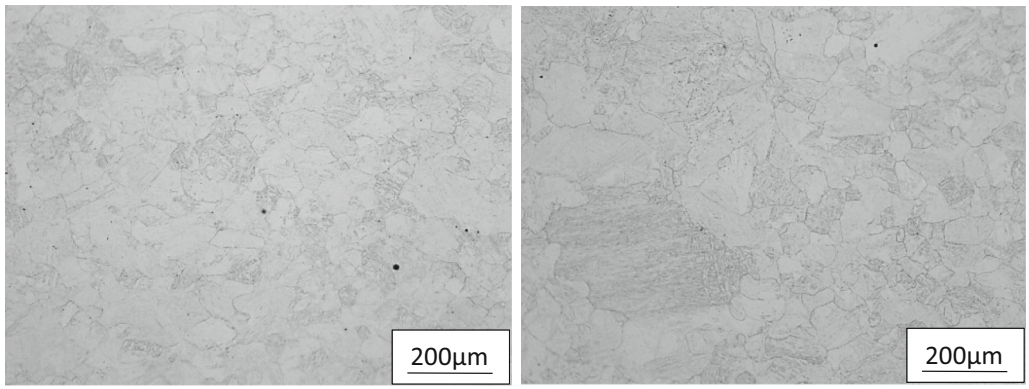

Fig. 6—Micrographs taken from samples deformed to 0.3 strain at 900 °C and held for 30 s before quenching: (*a*) homogenized sample showing a fine and uniform grain structure, and (*b*) segregated sample showing mixed coarse and fine grains.

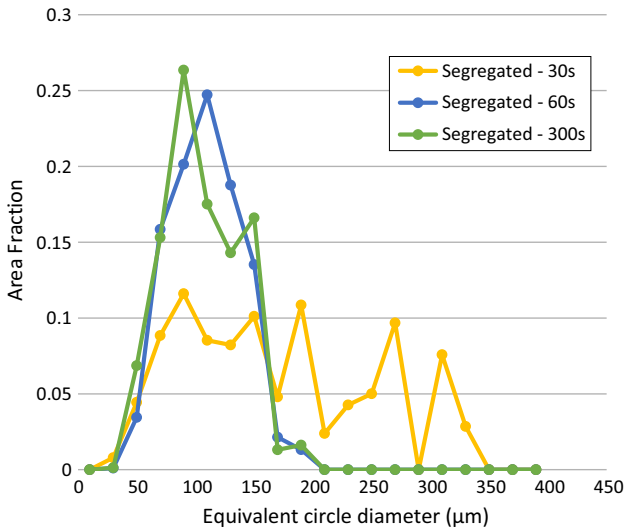

Fig. 7—Comparison between the austenite grain size of the segregated sample deformed at 900 °C to 0.3 strain and held for 30, 60, and 300 s.

segregated sample is partially recrystallized with some of the larger grains in the original distribution remaining, resulting in a much broader grain size range (20 to 340 μm) and no clear mode. This broad distribution comes from the smallest grains in the distribution recrystallizing first, and as such from even smaller grains. The larger grains, due to the reduced density of potential nucleation sites, recrystallize much later and, as such, remnants of the larger grains in the initial distribution can still be seen after a 30-second hold.

It should be noted that the initial grain size distributions (Figure 4) show that the homogenized sample has a slightly larger grain size, which would be expected to take a slightly longer time for 85 pct recrystallization than for the segregated sample (11 seconds compared to 8 seconds for the mode grain size); however, it is the segregated sample that has not fully recrystallized showing that the segregated composition has affected the recrystallization kinetics.

Further segregated samples were deformed at 900 °C and held for 60 and 300 seconds before quenching (Figure 7) to determine the effect of segregation on the recrystallization kinetics and the fully recrystallized grain size distribution. It can be seen from Figure 7 that the sample is fully recrystallized after the 300-seconds-hold time (potentially after 60 seconds where all the large grains from the initial distribution have disappeared as well as a more uniform distribution can be observed), with mode grain sizes, respectively, in the range of 80 to 100 μm and the range of 20 to 180 μm. The sample held for 60 seconds after deformation has a very similar grain size distribution, with a slightly higher number of large grains (120 to 140 μm) and lower number of fine grains (60 μm). This may be due to statistical sampling but could also indicate that full recrystallization has not quite been achieved. When comparing the final recrystallized grain structures in the segregated and homogenized samples, it can be seen that the homogenized sample has a tighter distribution (20 to 140 μm compared to 20 to 180 μm) and smaller mode size (62 μm compared to 92 μm).

Figure 7 shows that significant grain size refinement has taken place in the deformed segregated sample on holding for 60-seconds compared to the sample of 30-seconds hold, with a further small grain size refinement seen when holding for 300 seconds. The small grain size refinement for the longer hold time suggests that no grain growth is occurring, and that these values can be considered to be the true recrystallized grain size. In comparing the fully recrystallized homogenized sample (30 seconds) and segregated sample (300 seconds), it can be seen that the mode and largest grains are nearly 50 pct greater in the segregated sample, and this is likely to have implications for the final product as the prior austenite grain size affects the transformed microstructure. For example, this grade of steel is used for forged automotive components where the prior austenite grain size affects the martensite packet and lath size, which in turn influence the mechanical properties[20,21]: a larger mode packet and lath size

reduces the yield strength of the material, while a larger coarse (or bimodal) martensite packet and prior austenite grain size will cause large scatter in toughness.[22,23]

To obtain such a distinct difference between the homogenized and segregated sample distributions after 30-seconds-hold means that a significant difference in the global Rf time for the material must be present. As these steels are not microalloyed, and as such, they have no precipitates pinning the boundaries; thus, the differences between the two curves must be attributed to strain variations.

We can use Eq. [1] to predict the recrystallized grain sizes for three locations in the initial grain size distribution (10 pct, mode and 90 pct of the maximum grain size, referred to henceforth as D_{10}, D_{mode}, and D_{90}), and then predictions of the change in grain size distribution due to recrystallization can be made. The results are given in Table II. In the table, it can be seen that the homogenized sample shows reasonable agreement between the measured and predicted grain size values for the D_{10} and D_{90} grain sizes, noting that the value of D' in Eq. [1] was fitted for the mode grain size. The same D' value was used for the segregated sample as D' is reported to be a function of steel composition, strain, and grain size,[16,24] all of which are macroscopically the same in both samples. However, when looking at the differences for the segregated sample, much larger discrepancies can be seen. For the largest grains in the distribution (D_{90}), then the grains are nearly twice as large as predicted. As Eq. [1] has only two variables (strain and initial grain size), the reason for the difference between predicted and measured grain size must be attributed to the inhomogeneity of strain within the sample with some areas showing a reduced local strain resulting in slower kinetics of recrystallization and a larger recrystallized grain size.

IV. MODELING THE EFFECT OF SEGREGATION ON RECRYSTALLIZATION

Based on the compositional profile seen in Figure 3, a simple uniaxial compression test configuration was simulated using the multiphysics software COMSOL 5.3a. The materials yield strength was set as a function of the Mn content using Eq. [4].

$$\sigma_y = \sigma_o + (\text{im}(R, Z) \times \text{Mn} \times \text{SS}_{Mn}), \qquad [4]$$

where σ_y and σ_o are the resultant yield strength and the yield strength of pure iron, respectively. Mn is the wt pct of Mn, SS_{Mn} is the solution-strengthening coefficient for Mn, and im(R, Z) is the coordinate location of the image with reference to the COMSOL geometry. Values of 32 and 43 MPa/wt pct have been used for SS_{Mn}, which represents the range of values that have been reported for room-temperature Mn solid-solution-strengthening contributions in ferritic steels.[10] No reports for the solid-solution-strengthening contribution of Mn in austenite at elevated temperature have been found; therefore, an assumed value has been taken as a first approximation. Fleischer[25] showed that the dominating factor of composition on the solution strengthening was how the solute interacts with dislocations due to the atomic size misfit. It has also been reported that despite a fitted relationship, a strong correlation between the change in lattice spacing and yield strength ensues according to the following relationship[26,27]:

$$\frac{\Delta\tau}{\Delta c} = AG\varepsilon^{\frac{4}{3}}, \text{ where } \varepsilon \approx \frac{\left(\frac{\delta a}{a}\right)}{\delta c}, \qquad [5]$$

where c is the concentration, G is the shear modulus, A is a material constant, a is the lattice parameter, and τ is the yield strength.

Figure 8 shows the changes in volumes of FCC and BCC iron with varying Mn contents. Although the absolute values are different, it can be seen that the relative changes are very similar, and therefore it can be expected that the strain induced in the Fe matrix is similar for both structures, and thus using the same proportional strength difference should be a reasonable assumption. It should be noted that the model is not being used to predict absolute loads but the strain distribution, so the relative differences in strength are more important; hence, any changes due to temperature have also been ignored.

This analysis has only taken Mn into consideration. As mentioned previously, Cr is known to segregate to similar levels as Mn, but, has a much reduced impact on solid solution strengthening. This can be seen in Table III where although C and Si are more prolific solution strengtheners, their tendencies to segregate are low and their diffusion rates are high. Therefore, assuming them as having a uniform distribution is appropriate.

Another aspect to consider is the influence of cosegregation. Carbon will preferentially segregate to areas of high Mn and Cr contents due to the difference in lattice spacing. To understand the impact of this, then a DICTRA[28] simulation was produced. An initial condition was applied with the segregation of Mn and Cr as stated earlier with a uniform C composition across the 100 μm length scale (Figure 9(a)). The system was defined as fully FCC and held at 900 °C for 500 minutes to allow the C to diffuse. Figure 9(b) shows that the C preferentially cosegregates to the Mn-rich region with 0.179 wt pct as opposed to 0.173 wt pct in the Mn-poor region. This 0.006 wt pct difference in C equates to around a 2 MPa difference in yield strength and has a minimal impact compared to the 43 MPa difference resulting from the Mn solution strengthening.

Figure 10 shows the predicted local strain maps from a uniaxial compression test after an overall 0.3 strain for a homogenized sample and for a sample with a segregated Mn composition (taken from Figure 3) where local differences in yield strength are based on the measured compositional profile and Eq. [4] with solution-strengthening coefficients of 32 and 43 MPa/wt pct. The maps are presented for the central 5 mm of the sample to match with the area that was assessed microstructurally on the physical samples. It can be seen that due to the variation in local mechanical properties,

Table II. Predicted and Measured Prior Austenite Grain Sizes for the Homogenized and Segregated Samples Based on the Initial Distributions

	Segregated			Homogenized		
	Measured (μm)	Predicted (μm)	Difference (pct)	Measured (μm)	Predicted (μm)	Difference (pct)
D_{10}	52.0	40.6	−28	42.0	45.3	7
D_{mode}	92.0	55.4	−66	62.0	61.2	0
D_{90}	130.0	67.2	−93	84.0	74.9	− 12

The differences show how much larger the measured grain sizes are compared to the predicted grain sizes.

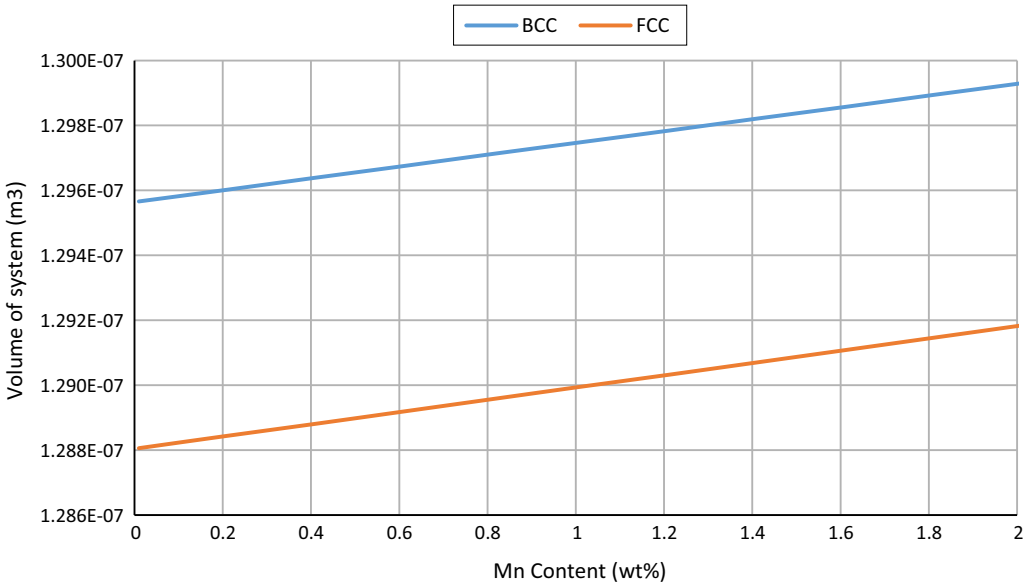

Fig. 8—Changes in volumes of BCC and FCC iron as a function of Mn content.

Table III. Summary of the Segregation Behaviors and Contributions to Solid Solution Strengthening for the Main Alloying Elements in the Presented Steel Grade

Element	Approx. Contribution to Solution Strengthening (MPa/Wt Pct)[10]	Segregation Tendency[28]	Diffusion Rate[28]
Mn	40	high	medium
Cr	5	high	medium
C	355	low	high
Si	60	low	medium/high

local strains with values in a range between 0.21 and 0.45 can be expected in the segregated sample when 32 MPa/wt pct was used, and strains in a range between 0.19 and 0.49 observed in samples under 43 MPa/wt pct. These values compare well with the homogenized sample where strains in the range of 0.26 to 0.35 were seen for both solution-strengthening coefficients. Using Eq. [1] and assuming that the largest grains in the recrystallized distribution have come from the largest grains in the initial distribution that have experienced the lowest strain (*i.e.,* 0.19), then a recrystallized grain size of 106 μm is predicted for D_{90} compared to 130 μm that was measured (Table IV). Although this still under-predicts the value observed, it is much closer than the value of 67 μm which is predicted for 0.3 strain assuming a homogenous strain distribution. Table IV shows that when the relevant strain variation (0.26 to 0.35) was applied to the homogenized sample, better agreement between grain sizes of D_{10} and D_{90} is seen than when using a uniform strain of 0.3 (given in Table II).

It is apparent, however, from Table IV that poor agreement is seen with D_{10} for the segregated sample. The following considerations are proposed to account for the lack of small grains seen in the recrystallized grain size distribution of the segregated sample:

- Because the high strain areas will recrystallize much faster than the low strain area, these newly recrystallized fine grains will be surrounded by areas of high

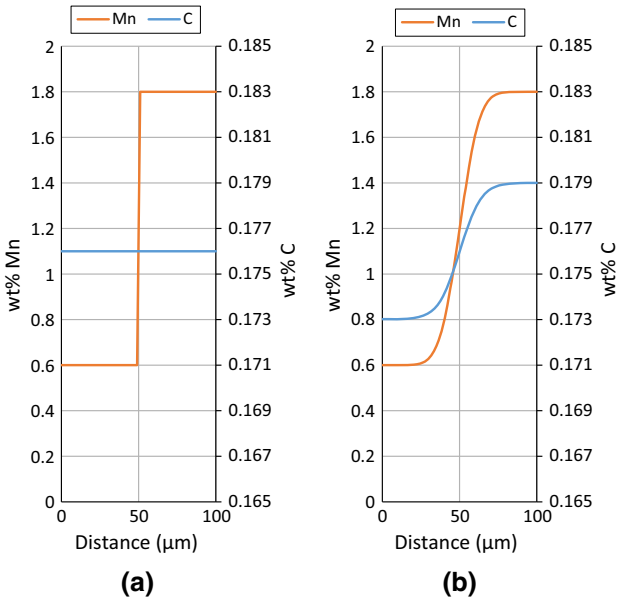

Fig. 9—Diffusion simulations showing the cosegregation of C to the Mn-rich regions. (*a*) Time 0 s of the simulations and (*b*) time 500 min at 900 °C.

stored energy. This may cause these fine recrystallized grains to grow into the low-strain areas until the low-strain areas start recrystallizing, resulting in a reduction in the number of small grains and also a shift in the mode grain size to a larger value, as seen in Table II.

- Predictions are based on a constant value for D'. It has been suggested that both grain size and strain can cause a variation in values of D' meaning that different D' values for the fine and coarse grains in a distribution are required.[16] This approach would need a full mapping of D' for both these parameters in order to more accurately predict the full distribution.

When using a uniform strain condition, Eq. [3] predicts an Rf of 11 seconds for the segregated sample; however, when using the strain value of 0.19 predicted in the high Mn region of the segregated sample, the Rf time is predicted to increase to 68 seconds. This agrees well with the experimental results which showed that at 60 seconds, almost complete recrystallization was seen in the segregated sample, and by 300 seconds, full recrystallization has occurred. This is an important approach, as this will help define the interpass times

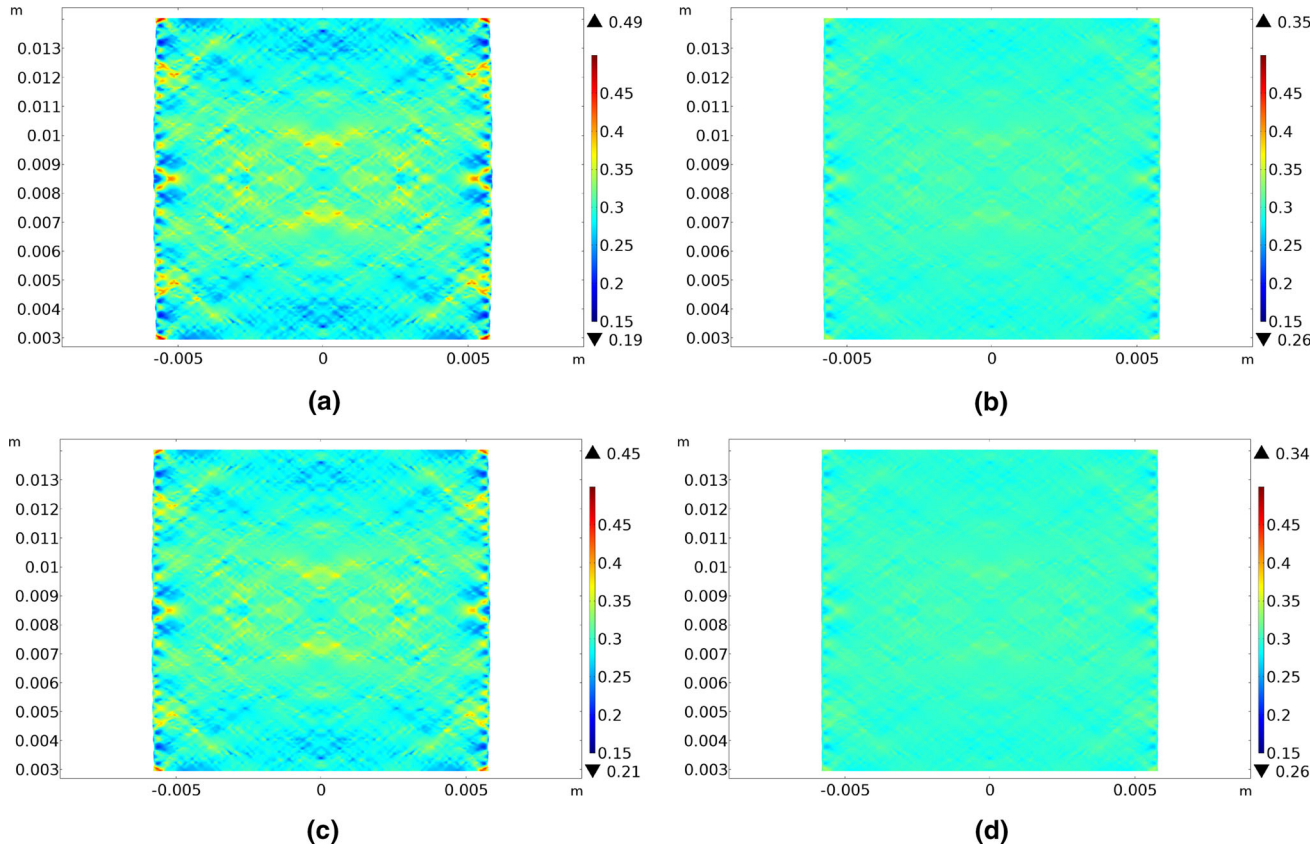

Fig. 10—Predicted strain distribution maps for the central 5 × 5 mm region of a uniaxial compression sampled tested to an overall 0.3 strain showing local deformation variations obtained using XRF mapping to give local changes in composition (Mn content) and therefore yield strength. (*a*) Segregated sample with 43 MPa/wt pct solution-strengthening coefficient, (*b*) homogenized sample with 43 MPa/wt pct solution-strengthening coefficient, (*c*) segregated sample with 32 MPa/wt pct solution-strengthening coefficient, and (*d*) homogenized sample with 32 MPa/wt pct solution-strengthening coefficient.

Table IV. Predicted D_{10} and D_{90} Grain Sizes for the Segregated and Homogenized Samples

	Segregated			Homogenized		
	Measured (μm)	Predicted (μm)	Difference (pct)	Measured (μm)	Predicted (μm)	Difference (Pct)
D_{10}	52.0	24.9	−109	42.0	40.0	− 5
D_{90}	130.0	106.1	−23	84.0	86.4	3

D_{10} was predicted assuming that the smallest grains will come from the smallest grains in the initial distribution coupled with the highest strains. D_{90} was predicted assuming that the largest grains in the new distribution will come from the largest grains in the initial distribution and a low-strain region.

needed in order to achieve full recrystallization and to avoid bimodality in the grain distribution. Even though the segregated sample produced a larger mode grain size, the distribution remained unimodal and as such the mechanical properties remain predictable.

The work presented in this paper shows the significance of segregation, in the case of Mn, on the recrystallization kinetics and the recrystallized grain structure. The impact due to this will be most pronounced where short interpass deformations allow just enough time for recrystallization to take place if a uniform strain exists. In this case, due to the increase in the time required for full recrystallization, a bimodal microstructure of coarse un-recrystallized grains and fine recrystallized grains may result. For cases where sufficient time for recrystallization occurs, then the level of refinement possible is much less when significant segregation is present giving a large mode and coarse grain sizes in the recrystallized grain size distribution, the effects of which will be to reduce both the yield stress and fracture toughness of the product.

V. CONCLUSIONS

In this study, the recrystallization kinetics and recrystallized grain size distribution in a C-Mn automotive forging grade steels in the as-received (90-mm-diameter bar stock) condition, containing a segregated compositional profile, and in the homogenized condition with the same initial grain size distribution, were examined. The segregated sample showed local variations in Mn content related to interdendritic segregation during casting from 0.6 to 1.8 wt pct in a banded distribution (band spacing approximately 200 μm) while the homogenized sample had a much reduced segregation variation (0.9 to 1.2 wt pct). The following observations have been made after carrying out uniaxial compression recrystallization experiments at 900°C:

1. After deformation to 0.3 strain and holding for 30 seconds, the homogenized sample showed complete recrystallization which resulted in a fine mode grain size (62 μm) and tight grain size distribution (20 to 140 μm). The segregated sample showed only partial recrystallization after holding for 30 seconds with many of the large grains in the initial distribution remaining un-recrystallized.
2. After a hold of 300 seconds, the segregated sample was fully recrystallized, with a 60-second hold also giving near-complete recrystallization. The recrystallized grain size range of the segregated sample was much broader (20 to 180 μm) with a coarser mode size (92 μm) than that of the homogenized sample.
3. Grain size predictions for the 10 pct, for mode, and for 90 pct grain sizes (D_{10}, D_{mode}, and D_{90}) in the distribution showed good agreement with measured values for the homogenized sample using a fitted D' value of 0.57 consistent with the literature. However, the segregated samples showed as much as a 93 pct discrepancy when comparing the predicted and measured largest grains in the distribution.
4. Predictions for the strain distribution due to the local yield strength variation, caused by compositional (Mn) segregation, were made using a simple FE model for uniaxial compression. For deformation of 0.3 strain, local strain variations between 0.19 and 0.49 are predicted due to the composition variations in the sample.
5. Assuming the larger grains in the recrystallized segregated sample came from areas of low strain with initially large grain size, then using a strain of 0.19 and the D_{90} of 254 μm from the initial distribution, the predicted final D_{90} of 106 μm is much closer to the measured 130 μm than the initial prediction of 62 μm based on uniform strain in a homogenized sample.

ACKNOWLEDGMENTS

The authors gratefully acknowledge the financial support by the Innovate UK for the innovative research project led by Jaguar Land Rover Ltd., TRANSCEND – TRANsmission Supply Chain Excellence for Next generation Dual clutch technologies (Reference 113061).

REFERENCES

1. J. Jonas: University of Wollongong Wollongong, 19841 J. Jonas: in *High Strength Low Alloy Steels*, Wollongong, Australia, 1984.
2. M.G. Akben, T. Chandra, P. Plassiard, and J.J. Jonas: *Acta Metall.*, 1984, vol. 32, pp. 591–601.
3. B. López and J.M. Rodriguez-Ibabe: *Microstructure Evolution in Metal Forming Processes*, Woodhead, Cambridge, 2012, pp. 67–113.
4. B. Dutta, E. Valdes, and C.M. Sellars: *Acta Metall. Mater.*, 1992, vol. 40, pp. 653–62.
5. B. Dutta and C.M. Sellars: *Mater. Sci. Technol.*, 1987, vol. 3, pp. 197–206.
6. M. Ji, V. Janik, M. Strangwood, and C. Davis: in *Proceedings of the 6th International Conference on Recrystallization and Grain Growth* (*ReX&GG 2016*), E.A. Holm, S. Farjami, P. Manohar, G.S. Rohrer, A.D. Rollett, D. Srolovitz, and H. Weiland, eds., Springer, Cham, 2016, pp. 153–58.
7. B.L. Ennis, C. Bos, M.P. Aarnts, P.D. Lee, and E. Jimenez-Melero: *Mater. Sci. Eng. A*, 2018, vol. 713, pp. 278–86.
8. A.G. Kostryzhev, C.D. Slater, O.O. Marenych, and C.L. Davis: *Sci. Rep.*, 2016, vol. 6, pp. 1–7.
9. R. Feng, S. Li, X. Zhu, and Q. Ao: *J. Alloys Compd.*, 2015, vol. 646, pp. 787–93.
10. D.T. Gawne and G.M.H. Lewis: *Mater. Sci. Technol.*, 1985, vol. 1, pp. 183–91.
11. K.-E. Thelning: *Steel and its Heat Treatment*, Butterworth-Heinemann, London, 1975, pp. 82–126.
12. D. Zhang: University of Birmingham, Birmingham, 2015.
13. B.C. De Cooman, Y. Estrin, and S.K. Kim: *Acta Mater.*, 2018, vol. 142, pp. 283–362.
14. Y.-M. Won and B.G. Thomas: *Metall. Mater. Trans. A*, 2001, vol. 32A, pp. 1755–67.
15. J.H. Beynon and C.M. Sellars: *ISIJ Int.*, 1992, vol. 32, pp. 359–67.
16. M.K.M. Kaonda: University of Birmingham, Birmingham, 2017.
17. M. Kosta, M. Kaonda, C. Slater, M. Strangwood, and C. Davis.
18. F. Wang, M. Strangwood, and C. Davis: in *SteelSim2015; 6th International Conference on Modelling and Simulation of Metallurgical Processes in Steelmaking*, Bardolino, Italy, 2015.
19. S.F. Medina and P. Fabregue: *J. Mater. Sci.*, 1991, vol. 26, pp. 5427–32.
20. S. Morito, H. Yoshida, T. Maki, and X. Huang: *Mater. Sci. Eng. A*, 2006, vols. 438–440, pp. 237–40.
21. T. Simm, L. Sun, S. McAdam, P. Hill, M. Rawson, and K. Perkins: *Materials (Basel)*, 2017, https://doi.org/10.3390/ma10070730.
22. D. Chakrabarti, M. Strangwood, and C. Davis: *Metall. Mater. Trans. A*, 2009, vol. 40A, pp. 780–95.
23. A.J. Kaijalainen, P.P. Suikkanen, T.J. Limnell, L.P. Karjalainen, J.I. Kömi, and D.A. Porter: *J. Alloys Compd.*, 2013, vol. 577, pp. S642–8.
24. M. Kaonda, C. Slater, M. Strangwood, and C. Davis: in *SteelSim2015; 6th International Conference on Modelling and Simulation of Metallurgical Processes in Steelmaking*, Bardolino, Italy, 2015.
25. R. Fleischer: *Acta Metall.*, 1963, vol. 11, pp. 203–209.
26. I. Toda-Caraballo: *Scr. Mater.*, 2017, vol. 127, pp. 113–17.
27. I. Toda-Caraballo, EI Galindo-Nava, and P.E.J. Rivera-Díaz-del-Castillo: *Acta Mater.*, 2014, vol. 75, pp. 287–96.
28. *Thermo-Calc Software. TCFE9 MOBFE3 ver 2019a*. Accessed 22 January 2019.